Relative humidity changes in a warmer climate

Steven C. Sherwood,[1,2] William Ingram,[3,4] Yoko Tsushima,[5] Masaki Satoh,[5,6] Malcolm Roberts,[7] Pier Luigi Vidale,[8] and Paul A. O'Gorman[9]

[1]   Key climate feedback due to water vapor and clouds rest largely on how relative humidity $\mathcal{R}$ changes in a warmer climate, yet this has not been extensively analyzed in models. General circulation models (GCMs) from the CMIP3 archive and several higher-resolution atmospheric GCMs examined here generally predict a characteristic pattern of $\mathcal{R}$ trend with global temperature that has been reported previously in individual models, including increase around the tropopause, decrease in the tropical upper troposphere, and decrease in midlatitudes. This pattern is very similar to that previously reported for cloud cover in the same GCMs, confirming the role of $\mathcal{R}$ in controlling changes in simulated cloud. Comparing different models, the trend in each part of the troposphere is approximately proportional to the upward and/or poleward gradient of $\mathcal{R}$ in the present climate. While this suggests that the changes simply reflect a shift of the $\mathcal{R}$ pattern upward with the tropopause and poleward with the zonal jets, the drying trend in the subtropics is roughly 3 times too large to be attributable to shifts of subtropical features, and the subtropical $\mathcal{R}$ minima deepen in most models. $\mathcal{R}$ trends are correlated with horizontal model resolution, especially outside the tropics, where they show signs of convergence and latitudinal gradients become close to available observations for GCM resolutions near T85 and higher. We argue that much of the systematic change in $\mathcal{R}$ can be explained by the local specific humidity having been set (by condensation) in remote regions with different temperature changes, hence the gradients and trends each depend on a model's ability to resolve moisture transport. Finally, subtropical drying trends predicted from the warming alone fall well short of those observed in recent decades. While this discrepancy supports previous reports of GCMs underestimating Hadley cell expansion, our results imply that shifts alone are not a sufficient interpretation of changes.

1.   Introduction

[2]   It is now widely known that the water vapor feedback in general circulation models (GCMs) is close to that which would result from a climate-invariant distribution of relative humidity [*Soden and Held*, 2006], as long anticipated before the advent of such models [e.g., *Arrhenius*, 1896; *Manabe and Wetherald*, 1967]. This sometimes gives the mistaken impression that models predict that relative humidity will remain invariant everywhere in warmer climates. In fact, several GCM studies have reported patterns of change in relative humidity [e.g., *Wetherald and Manabe*, 1980; *Mitchell and Ingram*, 1992]. These changes typically include a horseshoe-shaped pattern of relative humidity reduction in the tropical upper troposphere and the midlatitudes. While a similar pattern has been reported in a number of GCMs, we are not aware of any systematic evaluation or established explanation of it. In light of continuing uncertainties about water vapor and cloud feedback in GCMs [*Bony et al.*, 2006], it is worth investigating how robustly this pattern continues to hold in more recent GCMs, whether it can be explained physically, and whether it is consistent with observations. Only if we could answer yes to such questions could we be confident that model predictions were likely to be accurate.

[3]   While GCM-predicted changes in $\mathcal{R}$ are modest and of variable sign, thus not significantly affecting the global radiative feedback of water vapor [*Soden and Held*, 2006],

[1]Department of Geology and Geophysics, Yale University, New Haven, Connecticut, USA.
[2]Also at Climate Change Research Centre, University of New South Wales, Sydney, Australia.
[3]Met Office Hadley Centre, Exeter, UK.
[4]Also at Department of Physics, Oxford University, Oxford, UK.
[5]JAMSTEC Frontier Research Center for Global Change, Yokohama City, Japan.
[6]Center for Climate System Research, University of Tokyo, Tokyo, Japan.
[7]Met Office Hadley Centre, Exeter, UK.
[8]National Centre for Atmospheric Science, University of Reading, Reading, UK.
[9]Department of Earth, Atmospheric and Planetary Sciences, Massachusetts Institute of Technology, Cambridge, Massachusetts, USA.

this does not mean they are unimportant. First, changes in relative humidity that are small compared to the strong Clausius-Clapeyron dependence of saturation vapor pressure on temperature ($de_s/dT = 6$–18% K^{-1} depending on T) could still affect processes such as cloud formation or precipitation efficiency. In fact, a correspondence between patterns of $\mathcal{R}$ change and those of cloud cover change has been noted in the aforementioned GCM studies, with cloud changes driven by those of relative humidity [*Wetherald and Manabe*, 1980], indicating that the changes in $\mathcal{R}$ may have important indirect effects on radiative transfer. We will show that this remains true in the more recent Coupled Model Intercomparison Project (CMIP3) models. Also, observational and modeling results show that the behavior of convective precipitation is sensitive to relative humidity in the free troposphere [e.g., *Redelsperger et al.*, 2002], although this may not be well represented in GCM convective schemes [e.g., *Derbyshire et al.*, 2004]. Thus changes in the pattern of $\mathcal{R}$ could directly influence that of precipitation, regardless of any impact on the global mean radiation budget.

[4] Another reason to take interest in the $\mathcal{R}$ changes is that uncertainty remains as to the ability of GCMs to reproduce certain global or regional climate changes, and $\mathcal{R}$ changes may provide a useful constraint. In particular, several studies have noted recently that observed poleward shifts of the subtropical and midlatitude jets, precipitation zones, and other measures of the latitudinal extent of the tropics or Hadley circulation appear to be underpredicted by GCMs [*Seidel et al.*, 2008; *Johanson and Fu*, 2009; *Lu et al.*, 2009] claim, however, that trends in tropopause characteristics can be explained by those of radiative forcing by greenhouse gases (including ozone). Paleoclimate studies also suggest surprising expansions of the Hadley cell in warmer climates [*Brierly et al.*, 2009]. The magnitude of such poleward shifts is important due to the regional hydrological changes they cause, which loom as a daunting climate-change impact on the flanks of current precipitation zones. Since relative humidity distributions are strongly controlled by dynamical fields rather than local temperatures [*Sherwood*, 1996a], changes in these are relevant; *Hu and Fu* [2006], for example, used the location of a threshold of observed outgoing radiation (determined largely by upper-tropospheric relative humidity) to identify widening of the Hadley cell. In examining humidity changes, we will quantitatively test how well they can be explained by expansion of the Hadley cell, poleward shifts of storm tracks, and raising of the tropopause.

2. Models

[5] We begin with 18 ocean-atmosphere GCMs from the CMIP3 archive of simulations for the IPCC Fourth Assessment in 2007, with dynamical oceans and CO_2 increasing at 1%/yr to doubling, hereafter referred to as AR4 models [*Intergovernmental Panel on Climate Change*, 2007]. The models used here are those that submitted the humidity fields needed for this study. We compare the model state averaged for 10 years from the time of CO_2 doubling with that of the first 10 years, dividing the change in relative humidity $\mathcal{R}$ by the change in global mean surface temperature to obtain a climate sensitivity $\mathcal{R}$ of relative humidity.

[6] Initial results from the AR4 models showed a clear dependence of the changes on model resolution, which motivated us to examine a few available climate-change runs conducted at higher resolutions. Each of these models is atmosphere-only and one is an aquaplanet. First, we include two Atmosphere-only General Circulation Models (AGCMs) based on the Met Office Unified Model: a slightly modified version of HadAM3 [*Ingram*, 2002] run at three different horizontal resolutions from 60 to 1600 km, with 19 vertical levels, in perpetual July; and NUGAM, a nonhydrostatic model initially based on the HadGEM1 AR4 model [*Johns et al.*, 2006], developed to 90 km resolution by the UK-HiGEM project [*Shaffrey et al.*, 2010] and then 60 km resolution by the UK-Japan Climate Collaboration, using 38 vertical levels. Although the first of these is modified from the original HadAM3 it will be denoted HadAM3 herein. Finally, we include results from a 14 km resolution, 58-vertical-level global aquaplanet simulation [*Miura et al.*, 2005] by the Non-hydrostatic ICosahedral Atmospheric Model (NICAM) [*Tomita and Satoh*, 2004; *Satoh et al.*, 2008]. In each of these models, different climates were simulated by prescribing uniform changes in ocean surface temperatures: $+2$ K (vs. 0) for NICAM, $+2$ K vs. -2 K difference for HadAM3, and two perturbed runs (-2 K and $+4$ K vs. 0) for NUGAM. All were based on at least 10 years of simulation time except HadAM3, which was based on 2 years, though each year showed similar $\delta\mathcal{R}$.

3. Results

3.1. GCM Simulations

[7] The mean $\mathcal{R}$ (Figure 1) and $\delta\mathcal{R}$ (Figure 2) patterns with latitude and height among the AR4 models are similar to those reported previously for individual models [e.g., *Wetherald and Manabe*, 1980]. The $\delta\mathcal{R}$ pattern in particular is qualitatively similar among all models (see Figure 3), including the high-resolution AGCMs, though not all place the maxima in the same places (shading in Figure 2 indicates where at least 16 of the 18 models agree on the sign of $\delta\mathcal{R}$). The near symmetry of the response above the boundary layer is interesting and indicates that it is unlikely to depend on the presence of continents or details of the surface warming pattern. The symmetry and robustness of the $\delta\mathcal{R}$ pattern suggests that it is caused by relatively simple physical/dynamical mechanisms.

[8] The largest $\mathcal{R}$ changes are increases around the extratropical tropopause and just above the tropical tropopause, each of which reaches $\sim 2\%$ or more per kelvin of warming. Negative $\delta\mathcal{R}$ occurs in a horseshoe-shaped region, including the midlatitude and tropical uppermost tropospheres. Zonal and model-mean $\delta\mathcal{R}$ (relative to mean $\mathcal{R}$) in the troposphere never exceeds $\sim 20\%$ of the relative change in local specific humidity at constant relative humidity according to the Clausius-Clapeyron equation, which ranges from 6 to 18% K^{-1} of local air temperature. Since $\delta\mathcal{R}$ is small and varies in sign, it is not surprising that the global water vapor feedback in GCMs is close to that expected under constant relative humidity [*Soden and Held*, 2006].

[9] A simple explanation of the $\delta\mathcal{R}$ pattern would be to ascribe it to upward and poleward expansion of the original $\mathcal{R}$ distribution associated with previously documented rising of the tropopause and poleward shifts of climate zones and
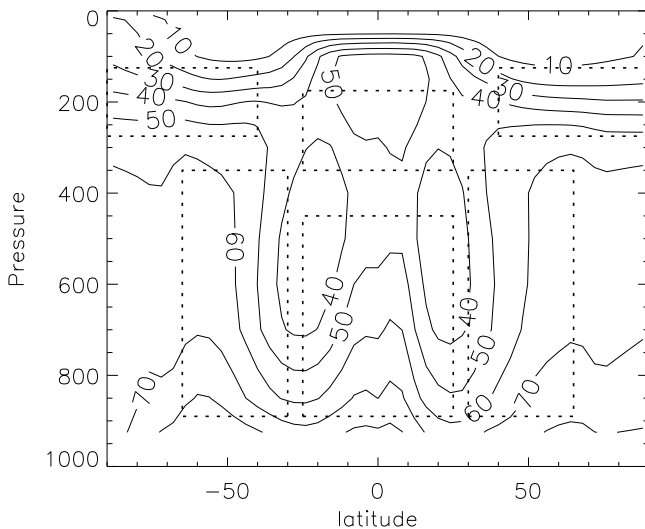
Figure 1. Mean $\mathcal{R}$ averaged over 18 AR4 model simulations of present-day climate. Dotted lines show averaging regions discussed in text: TL (25°S–25°N, 450–900 hPa); TU (25°S–25°N, 175–350 hPa); XL (30°–65°N/S, 350–900 hPa); XU (40°–90°N/S, 175–350 hPa).

circulation features. Indeed, regions of $\delta\mathcal{R} < 0$ coincide roughly with where $\mathcal{R}$ increases in the poleward (in the midlatitudes) or upward (below the tropical tropopause) directions and vice versa for the increase near and above the midlatitude tropopause. To explore the humidity changes, and this "shift" explanation in particular, more quantitatively, we examine means within the rectangular regions indicated in Figure 2, named TL, TU, XL, and XU for tropical-lower, tropical-upper, extratropical-lower, and extratropical-upper ones, respectively. (Data are interpolated to standard (mandatory reporting) pressure levels, these are averaged, and then zonal means are averaged with cosine-latitude weighting; averages for XL and XU include both hemispheres.) The TL and TU regions correspond to lower and upper parts of the tropical troposphere, while the XL is roughly the free troposphere in subtropical to midlatitudes, and XU spans the extratropical tropopause and lowermost stratosphere. To test the robustness of the results, we tried an alternative definition of these regions in which the box positions were adjusted for each model to locate over the region of strongest signal; this made the $\delta\mathcal{R}$ values on average about 20% stronger but did not qualitatively affect any of the relationships reported below.

[10] Figure 4 compares $\delta\mathcal{R}$ in each region to the relevant gradient $\nabla\mathcal{R}$ of $\mathcal{R}$ in the region, computed by taking the difference between $\mathcal{R}$ at the top and bottom (for the upper regions), two sides (XL region), or center and side (TL region) and dividing by the distance (in hectopascals or degrees). In each region except TL, $\delta\mathcal{R}$ and $\nabla\mathcal{R}$ vary roughly proportionally among the models. This correspondence is strongest in TU (Figure 4a), even holding for the models (save one) whose $\nabla\mathcal{R}$ is reversed from the average. This would be consistent with the changes being driven by a shift at a rate consistent across models—but see section 4.

[11] Meanwhile, Figure 5 shows that the magnitude of $\delta\mathcal{R}$ tends to increase with model horizontal resolution in

all four regions. This relationship is highly significant in all regions except TL, even among only the AR4 models ($p < 0.05$, assuming models are independent; if only half of the models were assumed independent, only the XU result would be significant at 95%). (Our use of two-sided tests for all regions is conservative, since once the relationship is established in one region and an anticipated sign of the response has been determined, a one-sided test would be sufficient to confirm that the same effect was occurring in other regions; this would halve the quoted p values for the other regions and allow TU to be significant at 95% even with a degree of freedom equal to only half the number of models.) In the extratropics (Figures 5b and 5d), results from all models suggest a plateauing or convergence once grid spacing falls below about 2°. This is supported not only by the AGCMs but also by the half dozen or so highest-resolution AR4 models and by the HadAM3 trend. All but one of the AGCMs are related and are thus not fully independent, so more high-resolution models would be needed to make a conclusive statement. Signals do not differ by more than ~20–30% between HadCM3 and the two NUGAM runs, suggesting that the response is mainly temperature driven and that interactive oceans and changing greenhouse gas concentrations (present in HadCM3 but not the AGCMs) do not play a major role. This also implies that details in the rate of warming (e.g., 1% per year vs. a more realistic 20th-century scenario) should not be important.

[12] In the tropics, the role of resolution is less clear. In the TL region, there is little correlation among different models, but the HadAM3 runs show $\delta\mathcal{R}$ increasing somewhat with model resolution. In TU the reverse is true: models generally show a correlation between $\delta\mathcal{R}$ and resolution (statistically significant at 95% even with only the AR4
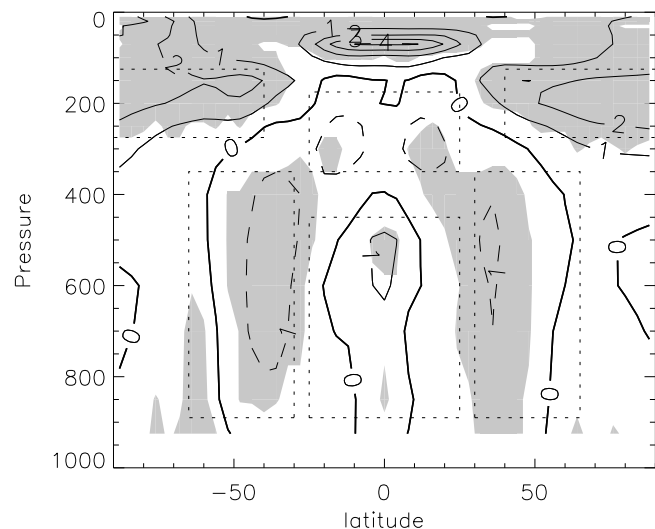
Figure 2. Change in $\mathcal{R}$ per Kelvin of surface warming averaged over 18 AR4 model simulations. Change found by computing the difference between $\mathcal{R}$ initially and at the time of CO_2 doubling and then dividing that by the simulated global mean temperature increase over the same time period. Solid/dashed contours are positive/negative. Shading shows regions where ~90% of models (at least 16 of the 18) agree on the sign of the change.
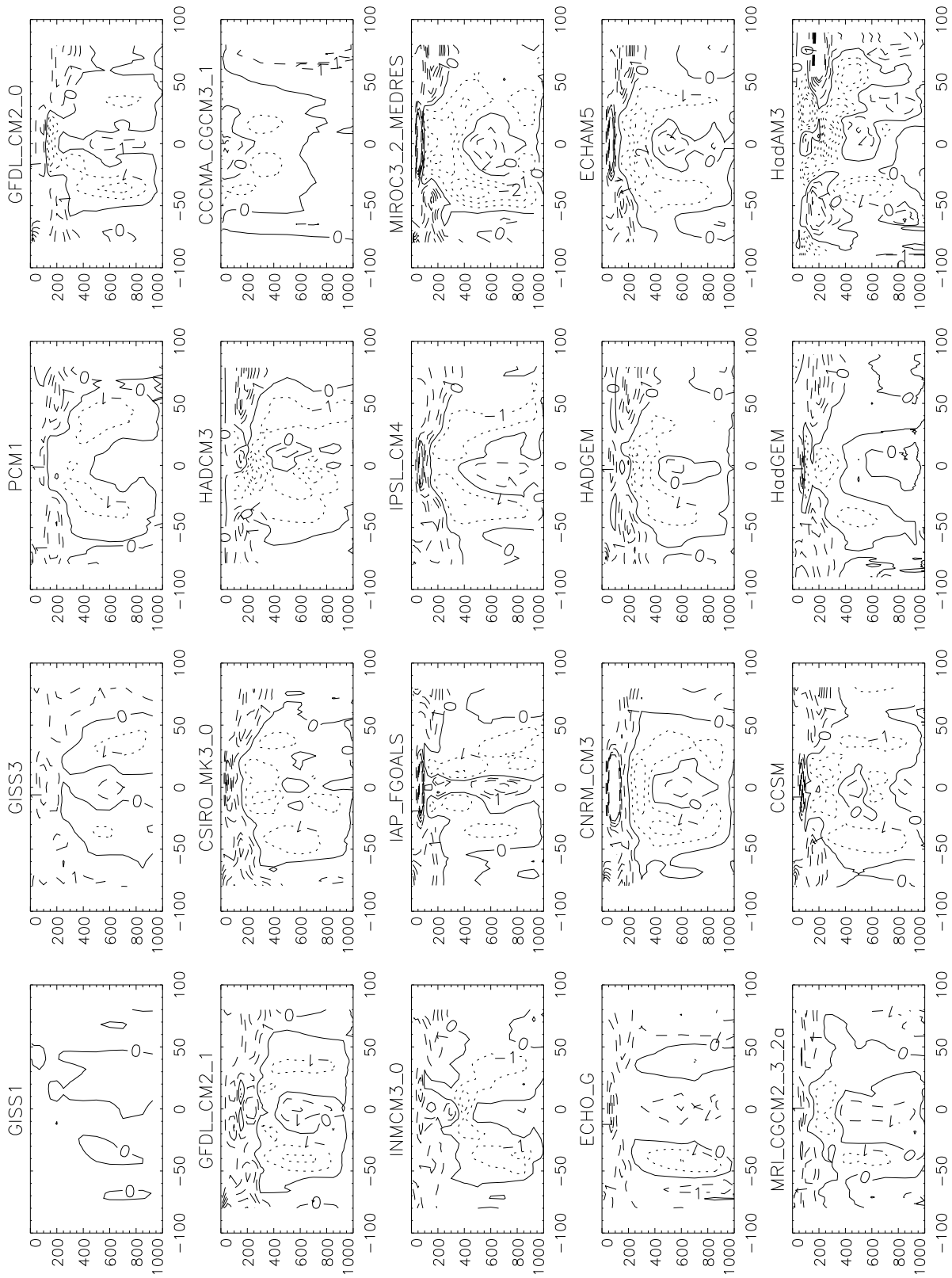
Figure 3. $\mathcal{R}$ for each individual model. Last two panels show the 60-km versions of HadGEM and HadAM3. The NICAM result, shown by *Miura et al.* [2005], is qualitatively similar to most of these.
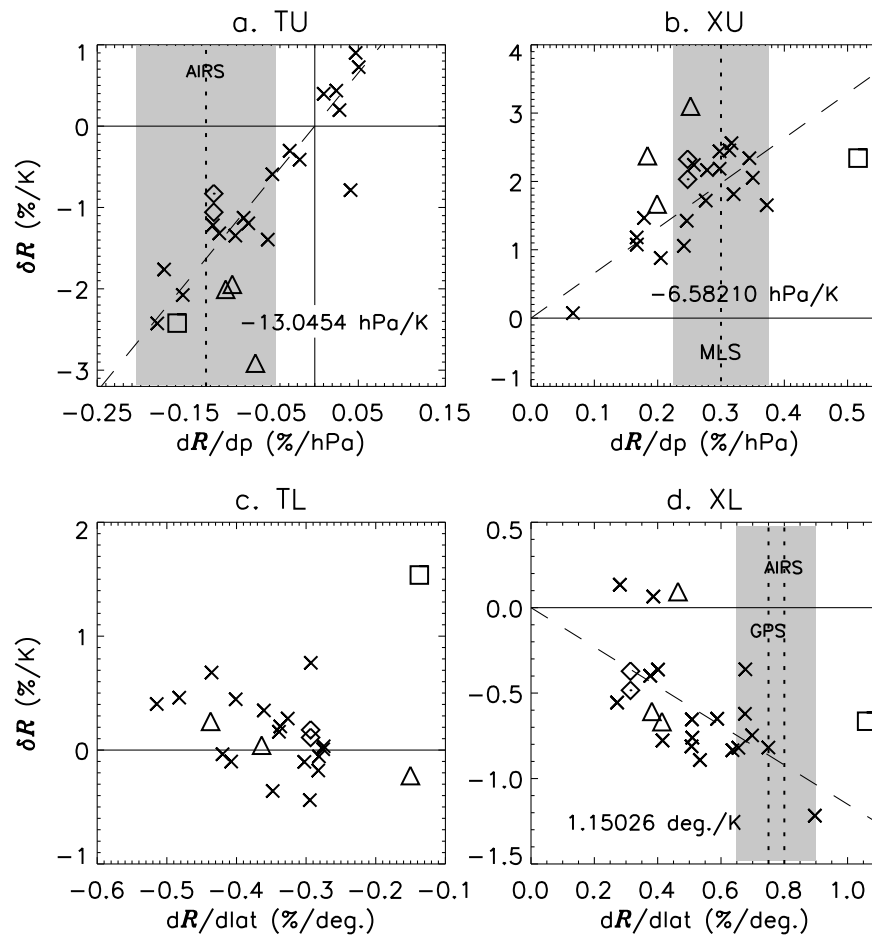
Figure 4. Change in $\mathcal{R}$ per kelvin of surface warming, averaged over four regions shown in Figures 1–2, plotted against (a, b) vertical or (c, d) horizontal gradient of $\mathcal{R}$. Cross, triangle, star, diamond, and square indicate AR4, HadAM3, HadCM3, NUGAM, and NICAM, respectively (see also Figure 5), with dotted diamonds indicating the NUGAM run with 2 K cooling. Dashed lines show best-fit linear relationships for the AR4 models, constrained to include the origin; slopes are printed in each panel. No fit is attempted in the TL region. Each observational estimate (see text) is shown by a dotted line, with shading indicating an uncertainty range.

models), but not HadAM3 at different resolutions. This suggests that other model characteristics (perhaps convective physics) are equally or more important in affecting tropical results. The low-resolution run of HadAM3 is an outlier in TU, having large $\delta\mathcal{R}$ despite low resolution and small $\nabla\mathcal{R}$. The reasons for this are unclear.

[13] We found no clear evidence of sensitivity to vertical resolution. Among the AR4 models, none of the signals here was related to the number of model levels (although this number is an imperfect index of tropospheric resolution). Furthermore, NUGAM signals were not stronger than those of HadAM3 despite NUGAM having twice as many levels. Since the number of tropospheric levels among AR4 models generally varies by less than a factor of 2, it is not surprising that no relationship was observed in that ensemble, and horizontal resolution appears to be the overriding factor though further studies of vertical resolution are warranted.

3.2. Comparison to Observations

[14] Observations are available to test a few of these signals. GPS data are well suited for measuring the latitudinal

gradient in the lower and middle troposphere in the current climate, as they are measured by the same instrument at different latitudes (thus minimizing spatially varying biases), have global coverage, are self-calibrated, and are unique among remotely sensed data in being essentially immune to cloud contamination [Hajj et al., 2004] that, if present, would cause significant latitude-dependent biases. We use the zonal means of GPS $\mathcal{R}$ distributions reported by Sherwood et al. [2006]. GPS can retrieve humidity consistently only for the first few kilometers in mid latitudes due to the sensitivity limitations of the instrument; we estimated the overall gradient in XL by multiplying that observed at 700 hPa by 0.8, a ratio taken from that exhibited by the GCMs (this is an average, but the ratio does not vary much among the models). The resulting estimate of the latitudinal gradient in XL matches that of the highest-resolution AR4 GCMs (see Figure 4d), an encouraging sign that the apparent convergence of the models is toward something realistic (similar results occur if we compare 700 hPa values from the GCMs and GPS). The gradient in NICAM is somewhat too strong, but as this model is simulating an aqua planet one should
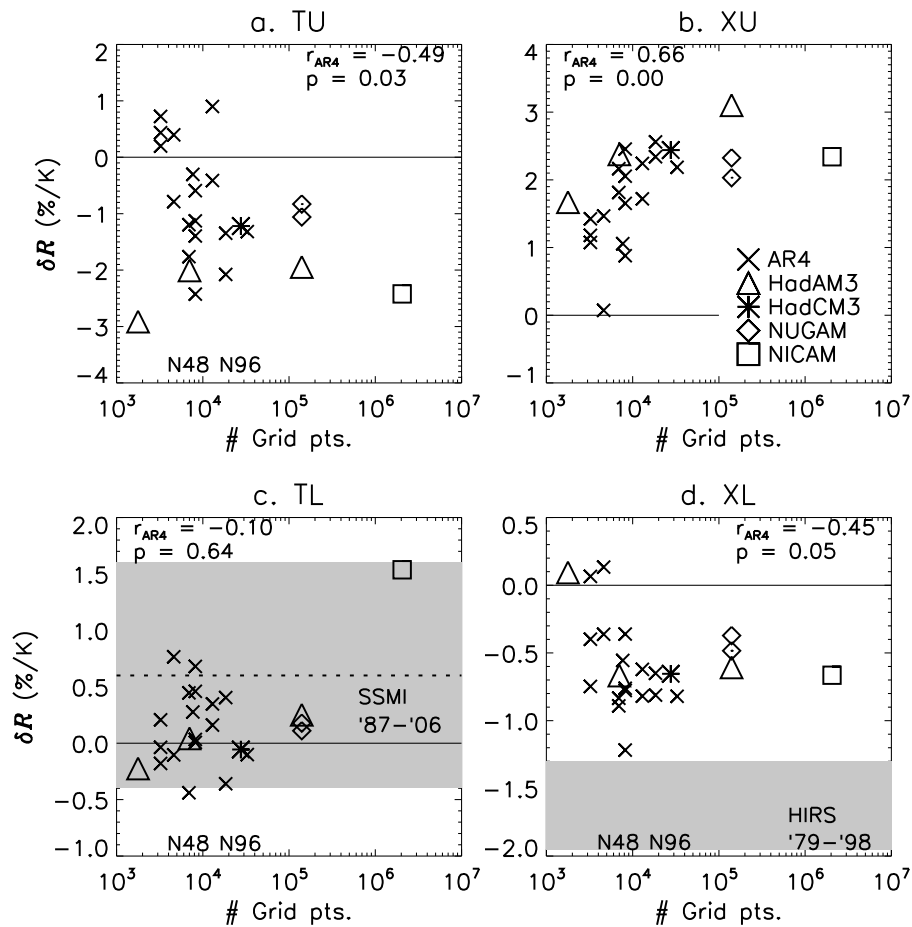
Figure 5. As in Figure 4 but plotted against the number of horizontal model grid points. Correlations and two-sided *p* values are shown for the AR4 models only. Such statistics, here and subsequently, are based on a standard normal model, with all data points (general circulation models) assumed independent unless otherwise stated. Central value for HIRS data, -3.3% K^{-1}, is off scale in panel d.

not expect its control humidity distribution to be quantitatively realistic.

[15] The Atmospheric Infrared Sounder (AIRS) also provides tropospheric humidity data. While subject to likely retrieval biases of order 10% or more [*Fetzer et al.*, 2008], this instrument can usefully observe to sufficient heights to cover our TU region. Here we present version 5 level 3 data for 2008 and assume 10% $\mathcal{R}$ uncertainty with uncorrelated error on opposite sides of a box. The vertical gradient in TU (see Figure 4a) is again similar to that of the higher-gradient GCMs. We also show the AIRS latitudinal gradient in XL, which is close to that of GPS (Figure 4d).

[16] We employ the more sensitive Microwave Limb Sounder (MLS) [see *Froidevaux et al.*, 2006] from the Aqua satellite (data Version 2.2x, annual mean from year 2007; results are identical for 2008) to assess the vertical gradient in the very dry XU region. This gradient is essentially determined by $\mathcal{R}$ at the 275 hPa level, where we again take an uncertainty of 10%. The gradient is again toward the high end of the AR4 models, though only ruling out the very weakest model gradients.

[17] Observations also place constraints, albeit limited, on some of the simulated trends. The TL region contains most

of the precipitable water (PW) in the tropics (and most of the remainder is in the lowest kilometer where $\mathcal{R}$ changes are very small), so trends in TL $\mathcal{R}$ should be detectable via the difference between an observed PW trend and that corresponding to constant relative humidity. *Wentz et al.* [2007] reported that tropical PW increased at 9.1% K^{-1} since 1987, to which we assign an uncertainty (based on the scatter in the data, not shown, provided by C. Mears) of $\pm 1.5\%$ K^{-1}. A calculation at constant $\mathcal{R}$ using an observed mean tropical radiosonde sounding and assuming a pseudoadiabatic warming profile yields 8.1% K^{-1}, although this number is somewhat sensitive to the relative humidity profile and assumptions made in calculating the adiabat. Taking 0.081 ± 0.0075 K^{-1} for $\partial \ln \mathrm{PW}/\partial T|_{\mathcal{R}}$ and subtracting this from the observed $d \ln \mathrm{PW}/dT$ yields a $d \ln \mathcal{R}/dT$ of 0.01 ± 0.017 K^{-1} or, since mean $\mathcal{R} \sim 60\%$ in TL, a $\delta \mathcal{R}$ of $0.6 \pm 1.0\%$ K^{-1} for this region. These mean and uncertainty estimates are approximate since not all precipitable water is in the TL region and $\delta \mathcal{R}$ is heterogeneous. They do not clearly exclude any model but provide some support for the positive $\delta \mathcal{R}$ in the TL (Figure 5c) shown by the majority of models.

[18] Matters are slightly better in the upper troposphere, where trends have been reported from the High-resolution

InfraRed Sounder (HIRS) for the years 1979–1998 [*Bates and Jackson*, 2001]. The reported UTH (upper tropospheric humidity) is a weighted mean of relative humidity from levels of roughly 250–560 hPa in midlatitudes, which includes the upper part of the XL region but may also be influenced by humidity nearer the tropopause (e.g., in XU). HIRS UTH is biased due to cloud clearing, but this bias (of order 20%) should be stable enough over time that changes in bias are small compared to the expected signal. Time trends reported by *Bates and Jackson* [2001] occurred in a pattern very similar to $\delta\mathcal{R}$ found here: moistening near the equator, midlatitude drying peaking near 40°N/S and somewhat stronger in the southern hemisphere, and slight moistening toward the poles. Averaging their values within our XL region yielded −0.5% per decade or about −3% K^{-1} if due entirely to the roughly 0.15 K per decade global-mean warming during the period. A 2-sigma error bar for this observation (based on errors given by *Bates and Jackson* [2001]) is shown in Figure 5d. The observed drying well exceeds that predicted in any of the GCMs as a consequence of warming, even though we have not accounted for the impact of UT/LS moistening on the UTH signal. Either most of the actual drying was not caused by warming per se, or the models are all significantly underestimating a key aspect of climate change (see section 7) even though many of them are getting the spatial gradients in today's climate about right. While erroneous drying in HIRS cannot be ruled out, calibration problems do not seem to fit as an explanation since the same instrument reports moistening at other latitudes of similar amplitude and the overall pattern qualitatively resembles predictions.

4. Evaluation of the "Shift" Explanation for Simulated $\delta\mathcal{R}$

[19] We now turn to possible explanations of the model behavior, in particular the "shift" idea noted earlier. For example, *Kushner et al.* [2001] found that most of the simulated wind and temperature changes in a warmed climate could be explained by simple shifts of the climatology. In view of the fairly linear relationships of the data in Figure 4, we infer an effective shift rate (in hectopascals per Kelvin or latitudinal degrees per kelvin) by taking the slope of the best-fit line through the origin, indicated by numbers in each panel. We then compare these to shift rates reported elsewhere based on indices of the circulation (winds, temperature, etc.).

4.1. Tropopause Lifting

[20] A CO_2-warmed climate exhibits a higher tropopause [*Santer et al.*, 2003] due to the contrast between the warming of the troposphere and the cooling of the stratosphere, which causes a tropospheric adiabat and a stratospheric radiative-equilibrium profile to intersect at a lower pressure. Thus if the upward displacement in the $\mathcal{R}$ pattern were directly associated with tropopause height change, we might have expected it to be weaker in the AGCMs (which lack changes in CO_2) than in the AR4 models. The data do not show this, however.

[21] In the XU region, the inferred rise rate of −6 to −7 hPa K^{-1} (Figure 4b) is ~30% greater than the ~4–5 hPa K^{-1} mean tropopause rise rate in the AR4 models [*Lu et al.*, 2007]; the spread of previously reported rise rates is also

similar to that of rates inferred here (about a factor of 2 from lowest to highest). Thus, a rising tropopause does seem to explain most of the $\delta\mathcal{R}$ signal in the extratropics, though perhaps not all.

[22] In the TU, the inferred rise rate, −13 hPa K^{-1}, is roughly 4 times the ~3 hPa K^{-1} average tropopause rise rate documented in the AR4 models [*Lu et al.*, 2007]. This confirms that tropopause lifting per se is not the main cause of drying in this region. As pointed out by *Hartmann and Larson* [2002], however, the height reached by convective overturning in the tropics tends to be tied to an isotherm below the tropopause where radiative cooling by water vapor becomes significant (not the cold-point tropopause). This suggests that the $\mathcal{R}$ pattern might track isotherms within the TU region, which rise faster (in hectopascals per kelvin) than the tropopause. But that would still only yield a shift rate of ~6 hPa K^{-1} based on the mean shift rates of isotherms in the TU region, only half that necessary to explain the drying in the GCMs.

4.2. Poleward Migration

[23] Poleward shifts of subtropical dry zones [*Previdi and Liepert*, 2007] and storm tracks [*Lu et al.*, 2008] have been reported in the AR4 models. Their cause is debated, and multiple mechanisms involving changes in either the lapse rate or tropopause height are possible [*Lu et al.*, 2008]. It has also been argued that they may not actually be caused by warming per se [*Lu et al.*, 2009] but by the direct radiative forcing of greenhouse gases.

[24] The poleward shift required to explain the XL signal, 1.15° latitude per kelvin on average, well exceeds the average expansion of the Hadley cell (0.3°–0.35° K^{-1} [*Previdi and Liepert*, 2007; *Lu et al.*, 2007]) or poleward retreat of the storm track (roughly 0.7° K^{-1} [*Lu et al.*, 2008]). This is also evident from examining (Figure 6) the 500 hPa $\mathcal{R}$ averaged over all models in the control climate and with 2 K of warming. The data at storm-track latitudes (near 45°N/S) are consistent with reported shifts of ~0.6°–0.7° K^{-1} on average, with data at higher latitudes suggesting little shift, but the curves near 30°–35°N (S) shift by 1° K^{-1} or more, which is at least 3 times the reported mean expansion rate. Also of interest, the NICAM aquaplanet produces a similar $\delta\mathcal{R}$ to other models of relatively high resolution, despite its $\mathcal{R}$ gradient being too strong (and the same happens in XU). Finally, the deepening of the subtropical minimum in $\mathcal{R}$ cannot result from a shift.

[25] Interestingly, this deepening occurs in all but three of the CGCMs but not in any of the AGCMs: changes in the latter are all less than 0.5% $^{-1}$, except for NICAM which shows a shallowing of 2% K^{-1}. This indicates that the deepening is not caused by the atmospheric warming per se but by the changes in the tropical SST pattern or increases in greenhouse gases that are absent in the AGCM runs. A cursory study revealed no significant relationships among the AR4 models between the amount of deepening and any identifiable feature of the tropical or equator-to-pole SST change, nor to changes in stratospheric cooling, so it remains unclear what exactly causes the deepening. However, this result may be relevant to the finding of *Lu et al.* [2009] that greenhouse gas increases can directly shift subtropical features poleward independent of tropospheric warming.
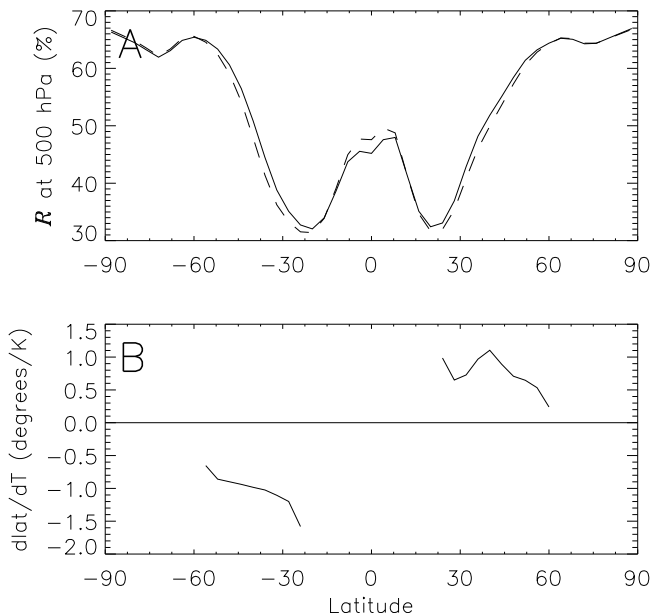
Figure 6. (a) Mean $\mathcal{R}$ at 500 hPa in the AR4 models in today's climate (solid line) and with 2 K of warming (dashed line). (b) Latitudinal shift rate required to account for the data in Figure 6a.

[26] As an additional test of whether shifting subtropics could still somehow account for the $\delta\mathcal{R}$ signal despite the evident mismatch in the expected and observed magnitude of the drying, we computed a multiple regression of $\delta\mathcal{R}$ in XL onto the two predictors $\nabla\mathcal{R}$ and δlat, the latter being the rate of expansion of the Hadley cell in each model according to *Previdi and Liepert* [2007]. The regression coefficient with $\nabla\mathcal{R}$ was highly significant ($p = 0.002$) while that with δlat was not statistically significant ($p > 0.1$). This argues against Hadley cell expansion as the primary cause of $\delta\mathcal{R}$.

5. An Alternative Explanation: Last-Saturation Temperature Changes

[27] Increased dryness has been noted in individual models and explanations have been put forward. For example, *Wetherald and Manabe* [1980] suggested that this may be due to increased variance of the vertical velocity due to stronger latent heat release with higher specific humidities. However, they concluded that this was not fully satisfactory, and more recent work suggests that higher specific humidities should, if anything, lead to weaker transient vertical motions [*Vecchi and Soden*, 2007; *O'Gorman and Schneider*, 2009]. *Mitchell and Ingram* [1992] argued that an elevated tropopause should lead to a drier troposphere but did not propose a quantitative model for this.

[28] We propose that the parts of $\delta\mathcal{R}$ not attributable to dynamical shifts may be explained by the nonlocal determination of $\mathcal{R}$ coupled with nonuniform changes of temperature as climate warms. Numerous studies show that specific humidity is determined approximately by the most recently experienced saturation value [*Sherwood*, 1996b; *Pierrehumbert and Roca*, 1998] so relative humidity is determined by the difference between current and last-saturation temperature and pressure. If last saturation (LS) events for a given target location tend to be far away, this allows $\mathcal{R}$ to change either because this distance changes or because the temperature difference between LS and target points change.

[29] Most air in the TU was last saturated in deep convective outflow regions, which tend to move upward as climate warms so that their temperature does not keep up with that in the upper troposphere itself. The resulting, negative $\delta\mathcal{R}$ was noted by *Mitchell and Ingram* [1992] and investigated more recently by *Minschwaner and Dessler* [2004] using a one-dimensional equilibrium mass-flux model. (Their study also analyzed observed variations, but these were dominated by El Niño–Southern Oscillation (ENSO), a poor analog for global warming [*Lu et al.*, 2008].) Predicted $\delta\mathcal{R}$ was large: roughly -5% K^{-1} of tropical convective-region SST, equivalent to at least -3% K^{-1} on the basis of the global-mean temperature according to typical GCM warming patterns. This is roughly twice the average $\delta\mathcal{R}$ in AR4 GCMs [see *Minschwaner et al.*, 2006]. While their simulated $d\mathcal{R}/dp$ (approximately 0.2%/hPa) was also large; it lies within the range of the GCMs, so their $d\mathcal{R}$ was larger than that implied by the linear relationship in Figure 4a. The GCM $\delta\mathcal{R}$ thus lies between that of a simple pattern shift and that predicted by a 1-D model. This is not too surprising given that the 1-D model treated convective detrainment as a source of saturated air free of condensate (thus with no reevaporation of condensate), ignored any vapor transports not required by the large-scale overturning and neglected subsequent condensation in the environment due to variable temperatures. Since these processes tend to act as moisture sinks that activate only at sufficiently high $\mathcal{R}$ (or sources that act only when it is low), one would expect them to have a stabilizing influence on $\mathcal{R}$ if accounted for.

[30] Air in the TL region was last saturated at higher levels in the troposphere [e.g., *Sherwood and Meyer*, 2006; *Dessler and Minschwaner*, 2007]. The tropical warming increases with height (approximating a moist adiabat), while the rate of reduction in $\mathcal{R}$ per K of parcel warming is less at higher temperature (from the C-C equation); both these robust and physically based effects will tend to make $\delta\mathcal{R} > 0$, barring changes in the circulation. Inserting a moist adiabatic lapse rate change (1% K^{-1}) and T^2 increase of 0.7% K^{-1} into the simple distribution of $\mathcal{R}$ calculated by *Sherwood et al.* [2006] yields a $\delta\mathcal{R} \sim 0.5\%$ K^{-1}, near the average GCM prediction. This could change by a factor of several with reasonable circulation changes due to the sensitivity of the result to small changes in the time scales involved [*Sherwood et al.*, 2006] and will depend on where last-saturation occurs, which may explain the lack of GCM consensus in this region.

[31] The most interesting region is the subtropics, where there is a definite (though variable) drying signal independent of Hadley cell expansion. Due to the steep slope of midlatitude isentropes, subtropical air often was last saturated near the extratropical tropopause [*Galewsky et al.*, 2005] where temperatures rise less than in the troposphere (or even fall) as climate warms. This would tend to push $\delta\mathcal{R}$ toward negative values, as could any diffusive or shallow-convective transport of water from near the surface where warming is also slightly slower. However, some last-saturation locations for tropospheric subtropical air also occur farther aloft in the tropics [*Dessler and Minschwaner*, 2007]; since
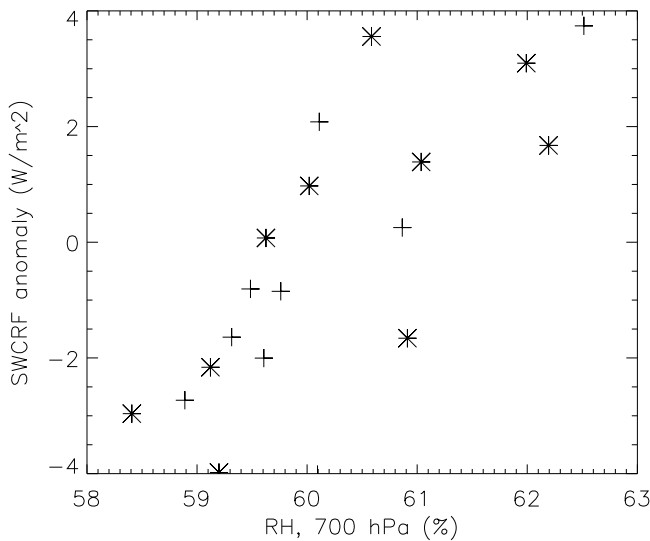
Figure 7. Relationship in one AR4 GCM (HadCM3) between interannual variations in cloud shortwave forcing (net reflection of sunlight to space) and relative humidity at 700 hPa in the Southern Hemisphere midlatitudes (30°–60°S) during December (asterisks) and February (plusses) of the first 10 years of the 1%/yr simulation.

warming rates increase with height in the tropics, this would tend to push $\delta\mathcal{R}$ toward positive values. Finally, to the extent that dehydration occurs locally, this should push $\delta\mathcal{R}$ toward zero if local temperature variability is not strongly climate sensitive. Thus we expect $\delta\mathcal{R}$ to be sensitive to where dehydration tends to occur in a particular model.

[32] One may also expect spatial gradients of $\mathcal{R}$ to be similarly affected. For example, if last saturation occurs geographically locally with relatively little unsaturated latitudinal transport, then climatological $\mathcal{R}$ might be relatively similar across latitudes; with robust diathermal transports of dry air, on the other hand, large latitudinal variations in $\mathcal{R}$ would become possible given the widely varying eddy regimes, for example, traversing the subtropical jet region. Such synoptic transports are likely to be more vigorous in models with horizontal grids capable of fully resolving them and do not appear to be easily resolved in at least some coarser models [*Bauer and Del Genio*, 2006]. A common rule of thumb in computational fluid dynamics (often forgotten in atmospheric modeling) is that one needs 10 grid points to resolve a feature; this would imply that to fully resolve synoptic eddies or jets of 1000 km scale would require a 100 km mesh, which roughly accords with the convergence resolution found here [see also *Orlanski*, 2008].

[33] In view of this argument, the correlations of $\delta\mathcal{R}$, $\nabla\mathcal{R}$, and model resolution found here are intriguing. The fidelity of moisture transports, and effects on $\mathcal{R}$ distributions and their climate sensitivity, are worthy of further investigation.

6. Effects on Clouds and Radiation

[34] Casual comparison of Figure 2 with Intergovernmental Panel on Climate Change–published changes in cloud cover in the same models [*Meehl and Stocker*, 2007, Figure 10.10] reveals detailed agreement between the patterns of change

in relative humidity and cloud cover above the boundary layer. Similarities in changes in these fields, noted in early GCM studies [e.g., *Wetherald and Manabe*, 1980], evidently persists today despite advances in cloud parameterization, although model averages mask some deviations in individual models due, for example, to cloud phase changes [*Tsushima et al.*, 2006]. Changes in $\mathcal{R}$ were similar when cloud cover was prescribed [*Wetherald and Manabe*, 1980], confirming that model cloud changes are mainly driven by $\mathcal{R}$ rather than the reverse. This is not surprising since cloudiness in models is typically predicted based at least in part on the local relative humidity. Such model physics should hold for trends as well as for smaller-scale variations.

[35] We regressed midlatitude (30°–60°S or N) monthly mean model cloud forcing onto $\mathcal{R}$ (separately for each month of the year) to estimate the impact on the global energy budget of a given change in midlatitude relative humidity. As this is the sum of long-wave and short-wave effects of opposite sign that each intensify with $\mathcal{R}$ (e.g., Figure 7), it is not surprising that there is no consensus among the AR4 models, with results ranging from −0.15 to +0.25 W m^{-2} per % RH. Given the decreases in annual mean $\mathcal{R}$ reported above of order 1% K^{-1} of surface warming for global warming simulations, this would imply feedback contributions of −0.15 to +0.25 W m^{-2} K^{-1} on global climate if the $\mathcal{R}$-cloud relationship held for warming. Similar positive feedbacks are likely through the UT/LS midlatitude cloud, due to the increases in humidity there. These would contribute significantly to overall cloud feedback, which ranges from roughly 0–1.0 W m^{-2} K^{-1} in the AR4 GCMs [*Soden and Held*, 2006].

[36] We expect that these cloud cover changes will be underestimated in models with insufficient resolution. Indeed, one recent climate simulation at very high resolution has produced an unusually strong increase in high cloud cover (Tsushima et al., unpublished manuscript, 2009). Although this particular result requires further analysis, it highlights the possibility that stronger feedbacks may become possible when synoptic motions are fully resolved. Having said this, we did not find either long-wave or short-wave global-mean cloud feedbacks to be significantly correlated with model resolution or $\delta\mathcal{R}$, but this does not rule out more subtle effects, including the effects of regional variations in cloud forcing or effects that require a resolution threshold to be reached. Clearly, the above calculations only scratch the surface, and much could be done to better understand how clouds and water vapor are related in models and observations.

7. Discussion and Conclusions

[37] We find that modeled changes in relative humidity ($\delta\mathcal{R}$) occur in a robust pattern but that their amplitude varies significantly. We have investigated this pattern quantitatively. In most places it varies in rough proportion to latitudinal or vertical gradients in the background $\mathcal{R}$ field. Outside the tropics, these gradients—hence, the $\mathcal{R}$ changes—correlate with model resolution. Many aspects cannot be evaluated with current observations, but horizontal $\mathcal{R}$ gradients appear to have converged and to be consistent with what observations there are, once model grids reach 2° or so. In models with coarser horizontal resolution, humidity fields are often too smooth and $\delta\mathcal{R}$ smaller. In particular, the low resolutions

(e.g., T31) typical of past global, coupled paleoclimate simulations are unlikely to properly capture humidity behavior. With predicted cloud changes driven by those of relative humidity, this may limit the ability of low-resolution models to correctly simulate regional climate feedbacks, although we find no evidence that global-mean cloud or water vapor feedbacks are resolution dependent.

[38] The $\delta\mathcal{R}$ pattern appears to result only partly from well-known upward and poleward expansions of simulated circulation features. Changes in the subtropics and below the tropical tropopause are 2–3 times too large for this explanation, and subtropical $\mathcal{R}$ minima deepen in all but a few coupled models under climate warming. We suggest that this is because air in these regions tends to have been last saturated elsewhere in locations that do not warm as fast, with this effect being stronger in models where synoptic transport across mean isothermal surfaces is more vigorous. A similar effect has been simulated for the tropical upper troposphere and would explain both the relation of $\delta\mathcal{R}$ to simulated climatological gradients and to model horizontal resolution. We have not tested this hypothesis directly, which ideally would exploit dedicated runs of a model equipped with suitable tracers of transport such as those of *Galewsky et al.* [2005].

[39] Our results are relevant to previous findings that "widening of the tropics" (poleward shift of subtropical features) is several times too weak in models compared to observations [*Seidel and Randel*, 2007], that the observed trends appear to lie well outside modeled decadal variability [*Johanson and Fu*, 2009], but that the discrepancy could be due to under prediction of direct radiative forcing of ozone or CO_2 changes [*Lu et al.*, 2009]. We also find that predicted, warming-induced trends in subtropical $\mathcal{R}$ are several times too small, corroborating that a discrepancy exists—but we also find that the model trends are due mostly to mechanisms other than tropical widening. This complicates the discussion and suggests a possible link between the mechanisms controlling tropical widening and dehydration, even if the observed trend is not due to warming. Radiative forcings that cool the stratosphere as the troposphere warms, thereby driving circulation changes, could also contribute independently to $\delta\mathcal{R}$ by cooling the regions where some air is dehydrated, so we cannot rule out this explanation for the discrepancy. Further work should investigate controls on subtropical moisture and their possible connections to the Hadley cell characteristics—especially since reductions in subtropical relative humidity may directly or indirectly enhance the regional precipitation and/or cloud changes caused by shifting climate zones.

References

Arrhenius, S. (1896), On the influence of carbonic acid in the air upon the temperature of the ground, *Philos. Mag.*, *41*, 237–276.

Bates, J. J., and D. L. Jackson (2001), Trends in upper-tropospheric humidity, *Geophys. Res. Lett.*, *28*, 1695–1698.

Bauer, M., and A. D. Del Genio (2006), Composite analysis of winter cyclones in a GCM: Influence on climatological humidity, *J. Clim.*, *19*, 1652–1672.

Bony, S., et al. (2006), How well do we understand and evaluate climate change feedback processes?, *J. Clim.*, *19*, 3445–3482.

Brierly, C. M., A. V. Fedorov, Z. Liu, T. D. Herbert, K. T. Lawrence, and J. P. La Riviere (2009), Greatly expanded tropical warm pool and weakened Hadley circulation in the early Pliocene, *Science*, *323*, 1713–1718.

Derbyshire, S. H., I. Beau, P. Bechtold, J.-Y. Grandpeix, J.-M. Pirou, J.-L. Redelsperger, and P. Soares (2004), Sensitivity of moist convection to environmental humidity, *Q. J. R. Meteorol. Soc.*, *130*, 3055–3079.

Dessler, A. E., and K. Minschwaner (2007), An analysis of the regulation of tropical tropospheric water vapor, *J. Geophys.Res.*, *112*(D10), 120.

Fetzer, E. J., et al. (2008), Comparison of upper tropospheric water vapor observations from the microwave limb sounder and atmospheric infrared sounder, *J. Geophys. Res.*, *113*, D22110, doi:10.1029/2008JD010000.

Froidevaux, L., et al. (2006), Early validation analyses of atmospheric profiles from EOS MLS on the Aura satellite, *IEEE Trans. Geosci. Remote Sens.*, *44*, 1106–1121.

Galewsky, J., A. Sobel, and I. Held (2005), Diagnosis of subtropical humidity dynamics using tracers of last saturation, *J. Atmos. Sci.*, *62*, 3353–3367.

Hajj, G. A., C. O. Ao, B. A. Iijima, D. Kuang, E. R. Kursinski, A. J. Mannucci, T. K. Meehan, T. P. Y. L. J. Romans, and M. de la Torre Juarez (2004), CHAMP and SAC-C atmospheric occultation results and intercomparisons, *J. Geophys. Res.*, *109*, D06109, doi:10.1029/2003JD003909.

Hartmann, D. L., and K. Larson (2002), An important constraint on tropical cloud–climate feedback, *Geophys. Res. Lett.*, *29*(20), 1951, doi:10.1029/2002GL015835.

Hu, Y., and Q. Fu (2006), Observed poleward expansion of the Hadley circulation since 1979, *Atmos. Chem. Phys.*, *7*, 5229–5236.

Ingram, W. J. (2002), On the robustness of the water vapor feedback: GCM vertical resolution and formulation, *J. Climate*, *15*, 917–921.

Intergovernmental Panel on Climate Change (2007), *Working Group I: The Physical Science Basis of Climate Change*, Cambridge University Press, New York.

Johanson, C., and Q. Fu (2009), Hadley cell widening: Model simulations vs. observations, *J. Clim.*, *22*, 2713–2725.

Johns, T. C., et al. (2006), The new Hadley Centre Climate Model (HadGEM1): Evaluation of coupled simulations, *J. Clim.*, *19*, 1327–1353.

Kushner, P. J., I. M. Held, and T. L. Delworth (2001), Southern Hemisphere atmospheric circulation response to global warming, *J. Clim.*, *14*, 2238–2249.

Lu, J., G. A. Vecchi, and T. Reichler (2007), Expansion of the Hadley cell under global warming, *Geophys. Res. Lett.*, *34*, L06805, doi:10.1029/2006GL028443.

Lu, J., G. Chen, and D. M. W. Frierson (2008), Response of the zonal mean atmospheric circulation to El Niño versus global warming, *J. Clim.*, *21*, 5835–5851.

Lu, J., C. Deser, and T. Reichler (2009), Cause of the widening of the tropical belt since 1958, *Geophys. Res. Lett.*, *36*, L03803, doi:10.1029/2008GL036076.

Manabe, S., and R. T. Wetherald (1967), Thermal equilibrium of the atmosphere with a given distribution of relative humidity, *J. Atmos. Sci.*, *24*, 241–259.

Meehl, G. A., and T. F. Stocker (2007), Global climate projections, in *Working Group I: The Physical Science Basis of Climate Change*, pp. 747–845, Cambridge University Press, Cambridge, UK.

Minschwaner, K., and A. E. Dessler (2004), Water vapor feedback in the tropical upper troposphere: Model results and observations, *J. Clim.*, *17*, 1272–1282.

Minschwaner, K., A. E. Dessler, and P. Sawaengphokhai (2006), Multimodel analysis of the water vapor feedback in the tropical upper troposphere, *J. Clim.*, *19*, 5455–5464.

Mitchell, J. F. B., and W. J. Ingram (1992), Carbon dioxide and climate: Mechanisms of changes in cloud, *J. Clim.*, *5*, 5–21.

Miura, H., H. Tomita, T. Nasuno, S. Iga, M. Satoh, and T. Matsuno (2005), A climate sensitivity test using a global cloud resolving model under an aqua planet condition, *Geophys. Res. Lett.*, *32*, L19717, doi:10.1029/2005GL023672.

O'Gorman, P. A., and T. Schneider (2009), Scaling of precipitation extremes over a wide range of climates simulated with an idealized GCM, *J. Clim.*, *22*, 5676–5685.

Orlanski, I. (2008), The rationale for why climate models should adequately resolve the mesoscale, *High Res. Numer. Mod. Atm. Ocean*, Yokohama Inst Earth Sci, Springer, p. 29, proceedings of the International Workshop on High Resolution Modeling.

Pierrehumbert, R. T., and R. Roca (1998), Evidence for control of Atlantic subtropical humidity by large scale advection, *Geophys. Res. Lett.*, *25*(24), 4537–4540.

Previdi, M., and B. G. Liepert (2007), Annular modes and Hadley cell expansion under global warming, *Geophys. Res. Lett.*, *34*, L22701, doi:10.1029/2007GL031243.

Redelsperger, J. L., D. B. Parsons, and F. Guichard (2002), Recovery processes and factors limiting cloud-top height following the arrival of a dry intrusion observed during TOGA COARE, *J. Atmos. Sci.*, *59*, 2438–2457.

Santer, B. D., et al. (2003), Contributions of anthropogenic and natural forcing to recent tropopause height changes, *Science*, *301*, 479–483.

Satoh, M., T. Matsuno, H. Tomita, H. Miura, T. Nasuno, and S. Iga (2008), Nonhydrostatic icosahedral atmospheric model (NICAM) for global cloud resolving simulations, *J. Computat. Phys.*, *227*, 3486–3514.

Seidel, D. J., and W. J. Randel (2007), Recent widening of the tropical belt: Evidence from tropopause observations, *J. Geophys. Res.*, *112*, D20113, doi:10.1029/2007JD008861.

Seidel, D. J., Q. Fu, W. J. Randel, and T. J. Reichler (2008), Widening of the tropical belt in a changing climate, *Nature Geosci.*, *1*, 21–24.

Shaffrey, L., et al. (2010), UK-HiGEM: The new UK High Resolution Global Environment Model–Model description and basic evaluation, *J. Clim.*, *22*, 1861–1896.

Sherwood, S. C. (1996a), Maintenance of the free-tropospheric tropical water vapor distribution, Part I: Clear regime budget, *J. Clim.*, *9*, 2903–2918.

Sherwood, S. C. (1996b), Maintenance of the free-tropospheric tropical water vapor distribution, Part II: Simulation by large-scale advection, *J. Clim.*, *9*, 2919–2934.

Sherwood, S. C., and C. L. Meyer (2006), The general circulation and robust relative humidity, *J. Clim.*, *19*, 6278–6290.

Sherwood, S. C., E. R. Kursinski, and W. G. Read (2006), A distribution law for free-tropospheric relative humidity, *J. Clim.*, *19*, 6267–6277.

Soden, B. J., and I. M. Held (2006), An assessment of climate feedbacks in coupled ocean-atmosphere models, *J. Clim.*, *19*, 3354–3360.

Tomita, H., and M. Satoh (2004), A new dynamical framework of non-hydrostatic global model using the icosahedral grid, *Fluid Dyn. Res.*, *34*, 357–400.

Tsushima, Y., et al. (2006), Importance of the mixed-phase cloud distribution in the control climate for assessing the response of clouds to carbon dioxide increase: a multi-model study, *Climate Dyn.*, *27*, 113–126.

Vecchi, G. A., and B. J. Soden (2007), Global warming and the weakening of the tropical circulation, *J. Clim.*, *20*, 4316–4340.

Wentz, F. J., L. Ricciardulli, K. Hilburn, and C. Mears (2007), How much more rain will global warming bring?, *Science*, *317*, 233–235.

Wetherald, R. T., and S. Manabe (1980), Cloud cover and climate sensitivity, *J. Atmos. Sci.*, *37*, 1485–1510.

W. Ingram and M. Roberts, Met Office Hadley Centre, Exeter, UK.

P. A. O'Gorman, Department of Earth, Atmospheric and Planetary Sciences, Massachusetts Institute of Technology, Cambridge, MA 02139, USA.

M. Satoh and Y. Tsushima, JAMSTEC Frontier Research Center for Global Change, Yokohama City, Japan.

S. Sherwood, Climate Change Research Centre, UNSW, Kensington NSW 2052, Australia. (s.sherwood@unsw.edu.au)

P. L. Vidale, National Centre for Atmospheric Science, University of Reading, Reading, UK.